IPTC-18834-MS

Waterflood Performance Evaluation with Simple Tools: A Case Study of Sirikit Oil Field

S. Asawapayukkul, Chulalongkorn University; R. Laochamroonvorapongse, M. Pancharoen, Y. Rattanarujikorn, V. Tivayanonda, S. Palviriyachote, W. Sopitkamol, and P. Akrapipatkul, PTT Exploration and Production PLC

This paper was prepared for presentation at the International Petroleum Technology Conference held in Bangkok, Thailand, 14-16 November 2016.

Abstract

Waterflood has been long considered as a cost-effective way to significantly add worldwide reserves. Oil displacement by injected water is a main mechanism of waterflood; however, common factors including vertical heterogeneity, interwell connectivities, and lack of injection and production control lead to less-than-expected flood performance. The intensive data monitoring and interpretation are a key to understand ongoing flood performance. The case study of Sirikit oil field is a good example of waterflood in complex multilayer thin-bedded reservoirs.

The use of diagnostic plots and analytical tools were applied to investigate ongoing waterflood in different levels (area, reservoir, and well). The sweep efficiency plots were used to compare the waterflood efficiency among 13 different areas in Sirikit field. The impacts of key parameters including injection duration, pore volume injection, reservoir depositional environment, level of reservoir depletion when waterflood started, drive mechanism, and flood pattern on incremental recovery factor were scrutinized. In a reservoir level, the estimated recovery factor from production data, reservoir and fluid properties, and Modified-Y plot were compared to give more prudent numbers. The capacitance-resistance model (CRM) was selected to understand the travelling directions of injected water from production and injection data. In well level analysis, this study expands the vertical heterogeneity measurement from the use of core data to injection logging data via the Lorenz plots and the Dykstra-Parson coefficients to capture conformance effects. The vertical heterogeneity maps were constructed from calculated coefficients and well locations to shred some lights on the distribution of reservoir complexity. In addition, Hall's plot was selected to diagnose injection problems.

From analysis, the depositional environment plays an important role in sweep efficiency as areas with clastic braided reservoirs yield higher recovery gain from waterflood than areas with fluvio-deltaic reservoirs. The plots of recovery gain versus pore volume injection highlighted the areas with relatively poorer flood performance, which require further mitigation plans. The results suggest the sooner waterflood started, the higher recovery gain is anticipated. Waterflood in solution gas drive reservoir tends to yield higher incremental recovery gain from waterflood than gas cap drive reservoir. The recovery factor calculated from analytical methods confirms the numbers estimated from a decline curve analysis method.

CRM indicates that most injected water (70% to 100%) flows toward producers, which shows good interwell connectivities. The well analysis suggests the spatial distribution of moderate to high vertical heterogeneity. Hall's plots indicate that the 70% of total injectors have experienced injection problems mainly from plugging.

These insights are critically beneficial for future waterflood screening and evaluation, reservoir management, well conformance control, and injector treatment. This quick analysis will assist not only the waterflood performance improvement but also the future EOR decisions.

Introduction

The basic concept of waterflood is an oil displacement by injected water toward producers. Therefore, reservoir continuity, vertical heterogeneity, and injection-production control become key components of a successful waterflood project. Evidently, the comprehensive review of reservoir complexity and ongoing flood performance as well as the well-planned program of surveillance and monitoring are inevitable.

Lake (2010) states that the nature of reservoir deposition and diagenesis creates the presence of reservoir heterogeneity, which usually has the largest impact on vertical sweep efficiency. Sahni et. al (2005) compared the vertical heterogeneity estimation from core data and production logging tool (PLT) results and found that the larger investigation flow area of PLT tends to homogenize the sample heterogeneity.

Terrado et. al (2007) provided the practical surveillance and monitoring guildlines for field, block, pattern, and well levels and presented three case studies of El Trapial, Bangko, and Meren fields. From these principles, understanding field performance and identifying opportunities will improve hydrocarbon recovery.

This study aims to establish the systematic approach of spontaneous data monitoring and interpretation in different complex waterflood areas of Sirikit field. The study focuses on the comparison of waterflood performance among areas, the analysis of recovery efficiency in a reservoir level, and the investigation of injection conditions and vertical heterogeneity in a well level. First, the effects of reservoir and waterflood design parameters on recovery efficiency were studied. Second, reservoir level analysis was performed by integrating the results of analytical recovery factor, modified-Y plot, and CRM. Then, the evaluation of well injectivity by Hall's plots and estimation of vertical heterogeneity from ILT results by Lorenz and Dykstra-Parsons will be discussed.

Field Background

The Sirikit field is Thailand's largest onshore oil field and oil production started in December 1982. During an early phase, the production relies mainly on primary recovery with the assisted gas lift injection and pump installation. The pilot waterflood project was implemented in the EE area in 1989 before starting full-field implementation in several areas later. In 2015, the average field oil production is 29,000 STB/D, which is mainly contributed from 13 waterflood areas. In terms of geological information, two depositional environments include a fluvio-detaic system in D1, D2, and D3 reservoirs and a clastic braided system in SH1 and SH2 reservoirs.

Those waterflood areas can be categorized in terms of depositional environment, drive mechanism, well pattern, and waterflood maturity. (See more details in Table 1)

Table 1—Summary of Waterflood Areas in Sirikit Field

Project	Area	Reservoir	Depositional Environment	Drive Mechanism	Waterflood pattern	Timing When Waterflood Started	Cumulative Water Injection by Hydrocarbon Pore Volume
B	B	D3	Fluvio-Deltaic	Solution Gas	Peripheral	Jun-12	0.11
C	CC	D2	Fluvio-Deltaic	Gas Cap	Inverted 5 spot and Peripheral	Nov-10	0.33
	CC	D3	Fluvio-Deltaic	Solution Gas and Gas Cap	Inverted 5 spot and Peripheral	Nov-10	0.16
	CC1	D2	Fluvio-Deltaic	Gas Cap	Inverted 5 spot and Peripheral	May-09	0.30
	CC1	D3	Fluvio-Deltaic	Solution Gas and Gas Cap	Inverted 5 spot and Peripheral	May-09	0.17
	CF	D2	Fluvio-Deltaic	Solution Gas	Inverted 5 spot and Peripheral	Jan-11	0.22
	CF	D3	Fluvio-Deltaic	Solution Gas	Inverted 5 spot and Peripheral	Jan-11	0.21
E	EE	D2	Fluvio-Deltaic	Solution Gas and Gas Cap	No Pattern	Jul-95	1.33
	EE	D3	Fluvio-Deltaic	Solution Gas	No Pattern	Jul-95	1.28
	EK	D2	Fluvio-Deltaic	Solution Gas and Gas Cap	Peripheral	Oct-03	0.61
	EK	D3	Fluvio-Deltaic	Solution Gas	Peripheral	Oct-03	0.35
	EL	D2	Fluvio-Deltaic	Gas Cap	Line Drive	Nov-06	0.86
	EL	D3	Fluvio-Deltaic	Solution Gas	Line Drive	Nov-06	0.27
D	D	SH2	Clastic Braided	Solution Gas	Peripheral	Jan-00	1.74
W	WA	D1	Fluvio-Deltaic	Solution Gas	Peripheral	Mar-07	0.18
	WA	D2	Fluvio-Deltaic	Solution Gas	Peripheral	Mar-07	0.42
	WC	SH1	Clastic Braided	Solution Gas	Peripheral	Nov-03	0.85
	WDE1	SH1	Clastic Braided	Solution Gas	No Pattern	Jul-03	0.89
	WDE1	SH2	Clastic Braided	Solution Gas	No Pattern	Jul-03	0.93
	WDE2	SH1	Clastic Braided	Solution Gas	No Pattern	Jun-03	0.50
	WDE2	SH2	Clastic Braided	Solution Gas	No Pattern	Jun-03	1.27
T	TW	SH2	Clastic Braided	Solution Gas	No Pattern	Oct-01	1.78

Waterflood Performance Comparison

The recovery efficiency plot was used to compare waterflood performance among 13 areas, which have different depositional environments, drive mechanisms, well patterns, and waterflood maturation. The incremental oil from waterflood was calculated from cumulative oil production after water injection started at particular areas. The calculated recovery factor from waterflood enables the comparison of areas with different sizes of original oil-in-place.

In Figure 1, the plot of recovery efficiency and waterflood duration shows the increasing recovery with injection time and clastic braided reservoirs yield higher recovery gain from waterflood than areas with fluvio-deltaic reservoirs. This can be explained by higher energy in a clastic braided environment causes larger grain deposition with better well sorting. Less contrast of permeability and fewer clay contents in a clastic braided environment are expected to improve both microscopic and volumetric sweep efficiency. The cumulative water injection by hydrocarbon pore volume (Cum PVI) gives better insight of waterflood

maturity because it was estimated from the ratio of cumulative water injection volume to total movable hydrocarbon pore volume. In Figure 2, the recovery efficiency vs. Cum PVI confirms higher recovery factor from clastic braided reservoirs. The data points with less steep slope represent the areas that require more focus on waterflood improvement plans. To investigate the effects of reservoir depletion level on waterflood performance, the recovery efficiency at Cum PVI of 0.2 was compared. For D1-D3 reservoirs, waterflood was implemented when reservoir pressure dropped below bubble point pressure. Figure 3 shows that the earlier waterflood starts, the better flood efficiency is. This is because the high level of reservoir depletion below bubble point pressure creates the presence of free gas in reservoir, which leads to longer time for a fill-up period. For the displacement process in saturated reservoir, the oil bank displaces mobile gas and leave trapped gas, which redissolves in oil phase at usual waterflood pressure (Willhite, 1986). Due to high mobility of gas in front of oil bank, the oil production during a fill-up period is minor. For SH1 and SH2 reservoirs, the recovery factors are relatively higher because waterflood was implemented when reservoir pressure is still above bubble point pressure. In Figure 4, depletion drive reservoir tends to yield higher recovery factor gain from waterflood than gas cap reservoir. In the S1 field, the waterflood well patterns were chosen based on simulation results and, in Figure 5, the recovery plot versus well patterns shows an inconclusive trend.

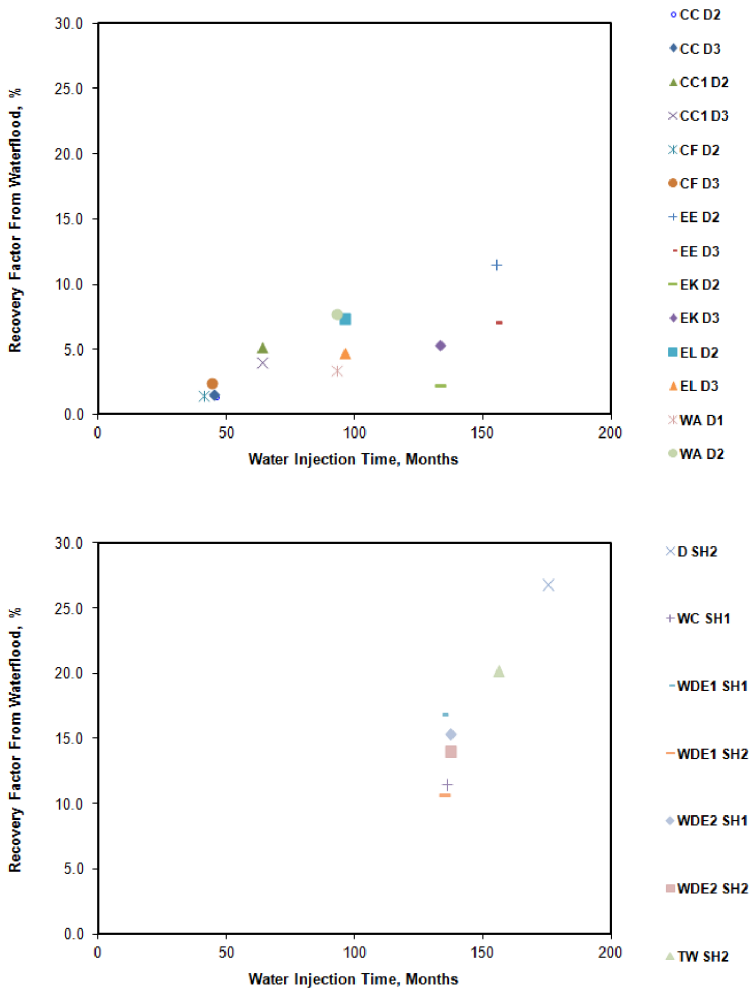

Figure 1—Recovery factor from waterflood vs. water injection duration for fluvio-deltaic reservoirs (top) and classic braided reservoirs (bottom).

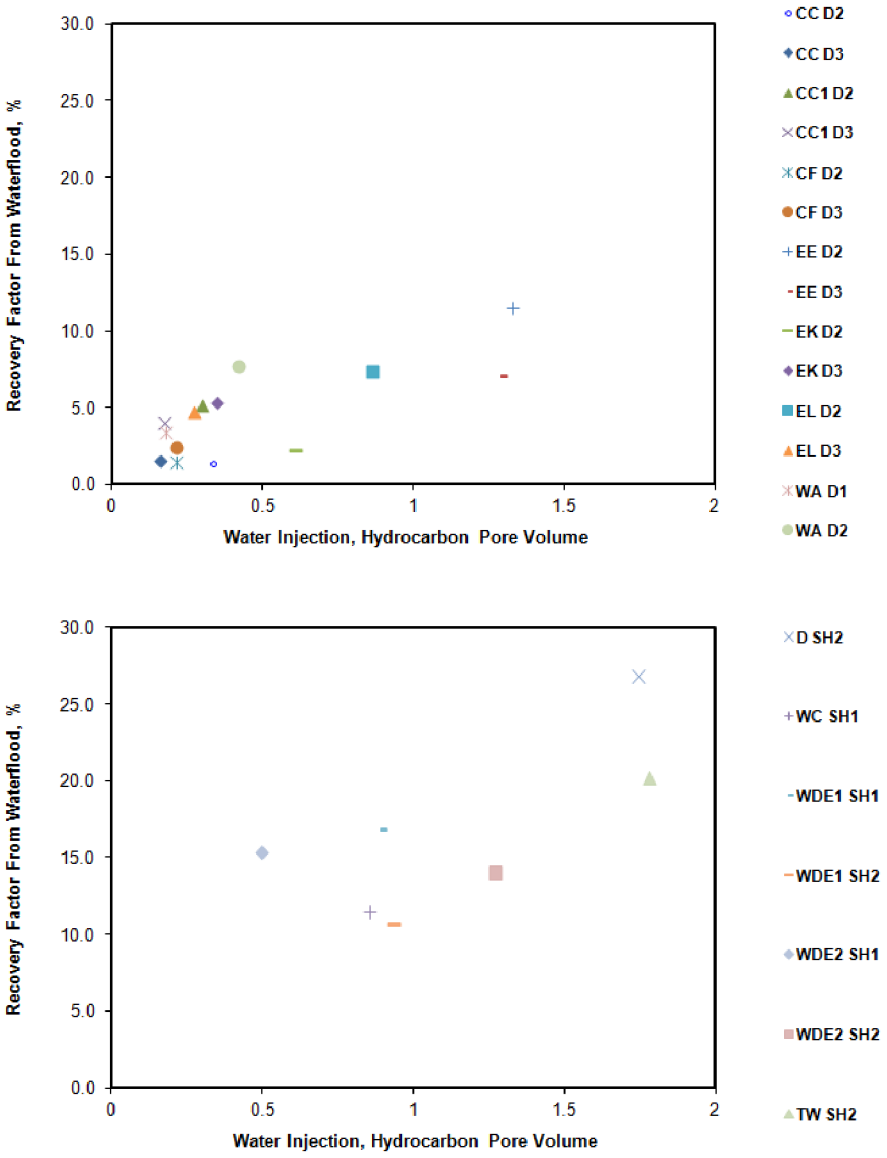

Figure 2—Recovery factor from waterflood vs. cumulative water injection by hydrocarbon pore volume for fluvio-deltaic reservoirs (top) and classic braided reservoirs (bottom).

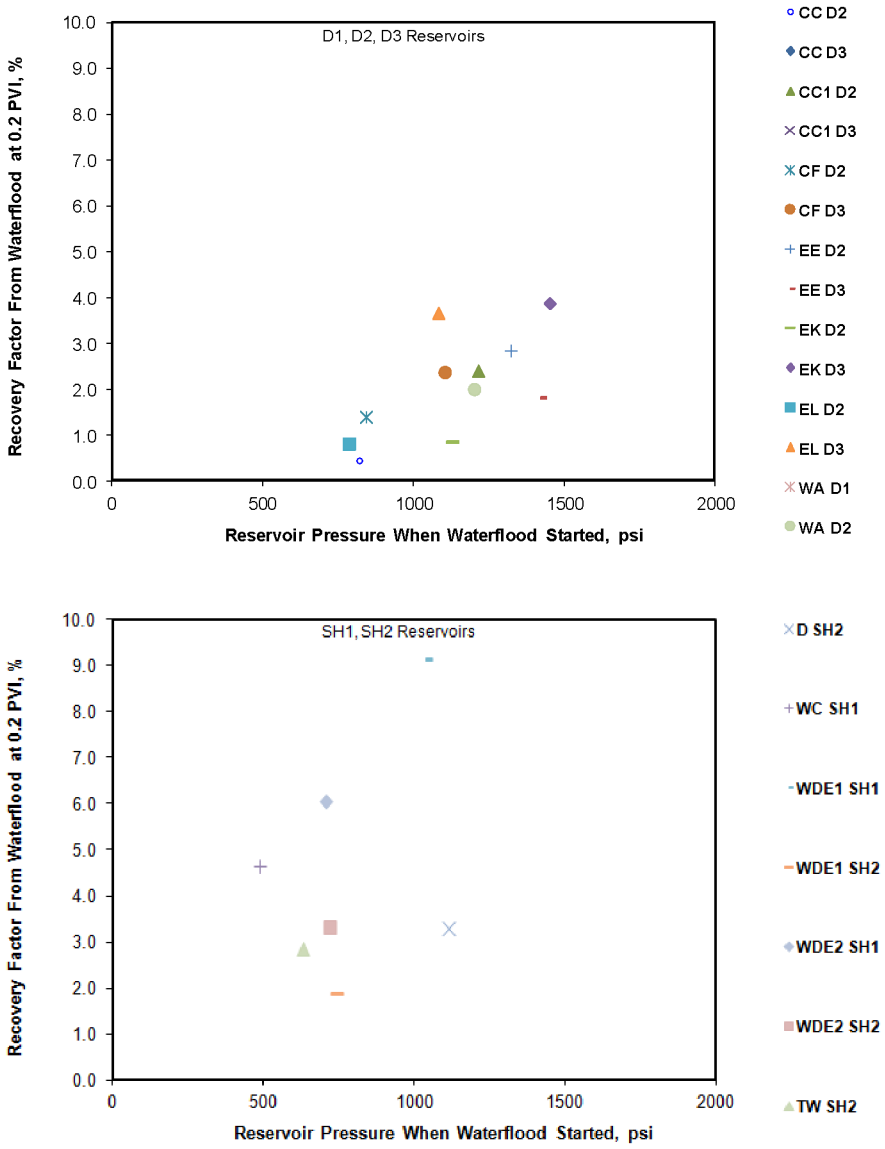

Figure 3—Recovery factor from waterflood at 0.2 PVI vs. reservoir pressure when waterflood started for fluvio-deltaic reservoirs (top) and classic braided reservoirs (bottom).

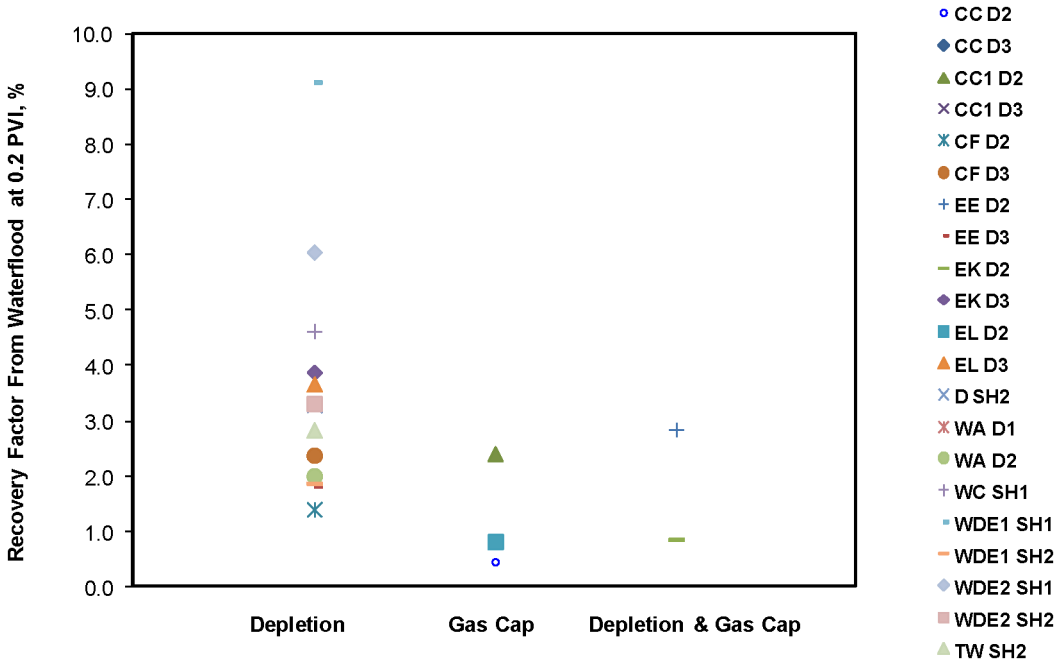

Figure 4—Recovery factor from waterflood at 0.2 PVI vs. reservoir drive mechanism.

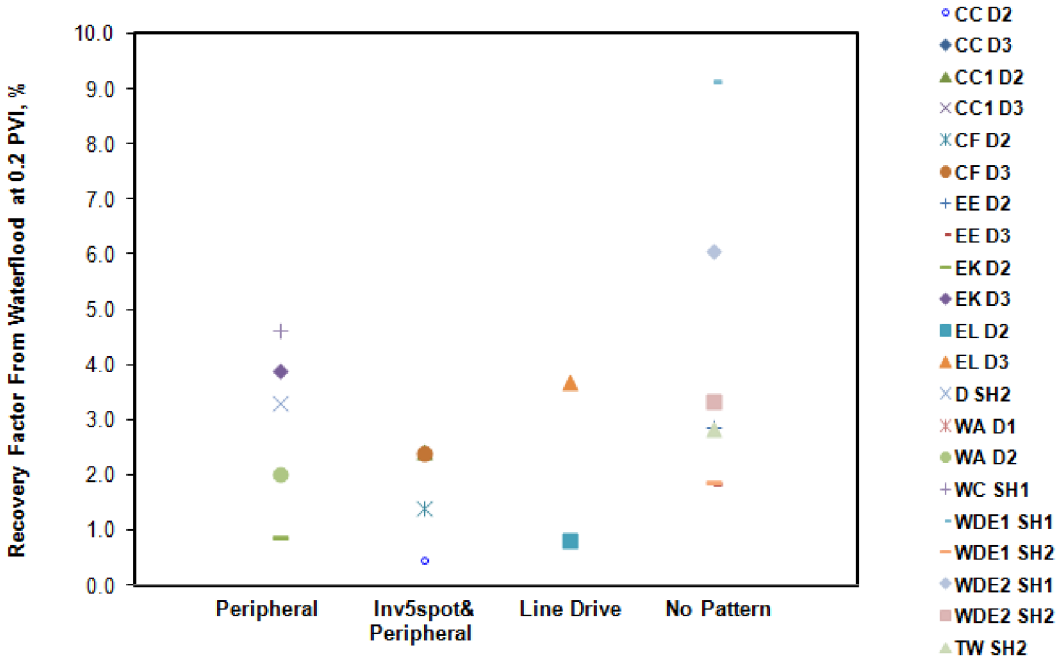

Figure 5—Recovery factor from waterflood at 0.2 PVI vs. well pattern.

Waterflood Performance Analysis

The detailed waterflood performance analysis was conducted by reservoir and well levels. Several analytical methods and diagnostic plots were applied to assess the relevant parameters related to flood efficiency.

Reservoir Level Analysis

The detailed analysis by reservoir level was performed in the EE area due to its high waterflood maturity. The recovery factor (E_r) is the product of microscopic (E_d), areal (E_a), and vertical (E_v) displacement efficiency as shown in Eq. (1). The available special core analysis (SCAL) data are a main input into the calculation of microscopic displacement efficiency, while the areal and vertical displacement efficiency

is estimated from the Fassihi type curves (Fasshi, 1986) based on calculated mobility ratio, vertical heterogeneity index (Dykstra-Parsons coefficient), and pattern type. The product of microscopic, areal, and vertical displacement efficiency (0.59 0.98) gives the recovery factor of 0.40. Craft and Hawkins (1991) mentioned the factors of interfacial tension, wettability, capillary pressure, and relative permeability affecting microscopic displacement efficiency. The capillary pressure plays an important role here as it illustrates the minimum pressure required to mobilize trapped oil in a pore system. Note that capillary pressure is a function of rock and fluid chemical composition, pore size distribution, and fluid saturation. In this case, the low microscopic displacement efficiency (0.59) is caused by relatively small grain sizes with high clay content leading to high capillary pressure. In addition, low vertical displacement efficiency is mainly due to high vertical heterogeneity as suggested by Dykstra-parsons coefficient of 0.7. The details of Dykstra-parsons method is presented in the next section. Very high areal sweep efficiency is directly due to favorable mobility ratio of 0.67.

$$E_r = E_d \times E_a \times E_v \tag{1}$$

Meanwhile, the modified-Y plot by Yang (2009), which was derived from the Buckley-Leverett equation, can be used to assess waterflood maturity and estimate volumetric sweep efficiency for a mature waterflood reservoir. As shown in Eq. 2, a log-log plot of Y and $1/t_D$ yields the slope value of $E_a\,E_v/B$ where t_D is the fraction of cumulative liquid production to related formation volume and B is the relative permeability ratio parameter. With the projection to water-oil ratio (WOR) cut-off, the recovery factor from waterflood can also be estimated. The example of modified-Y plot in the EE area is illustrated in Figure 6. The straight line can be established after reaching 0.33 pore volume injection. With the slope value ($E_a\,E_v/B$) of 1.46 and B value of 0.40, the estimated $E_a\,E_v$ is 0.58. Compared to volumetric sweep efficiency from the analytical method (0.98×0.70 or 0.69), the actual waterflood behavior is observed to be slightly worsened due to the existence of higher-than-expected reservoir heterogeneity. The extrapolation of Y and $1/t_D$ enables the estimation of oil cut with additional liquid production. With the field water-oil-ratio cut off at 49 bbl/bbl, the expected additional recovery factor (1.8%) and total recovery factor (31.9%) could be achieved. The total recovery factor was validated with the decline curve analysis (DCA) method, which the oil production data was fitted with exponential and hyperbolic decline trends. The comparison of total recovery factor among different methods is presented in Table 2.

$$Y = f_o(1 - f_o) = \left(\frac{E_a \times E_v}{B}\right)\frac{1}{t_D} \tag{2}$$

Table 2—Summary of Recovery Factor from Modified-Y Plots and DCA

Area	Block	Reservoir	Calculated B Value	Slope from Modified-YPlot (E_aE_v/B)	Calculated Volumetric Sweep Efficiency (E_aE_v)	Recovery Factor from Modified-Y Plot, %	Recovery Factor Estimated from DCA, %
E	EE	D2	0.40	1.46	0.58	32	32
	EE	D3	0.40	1.60	0.64	23	22

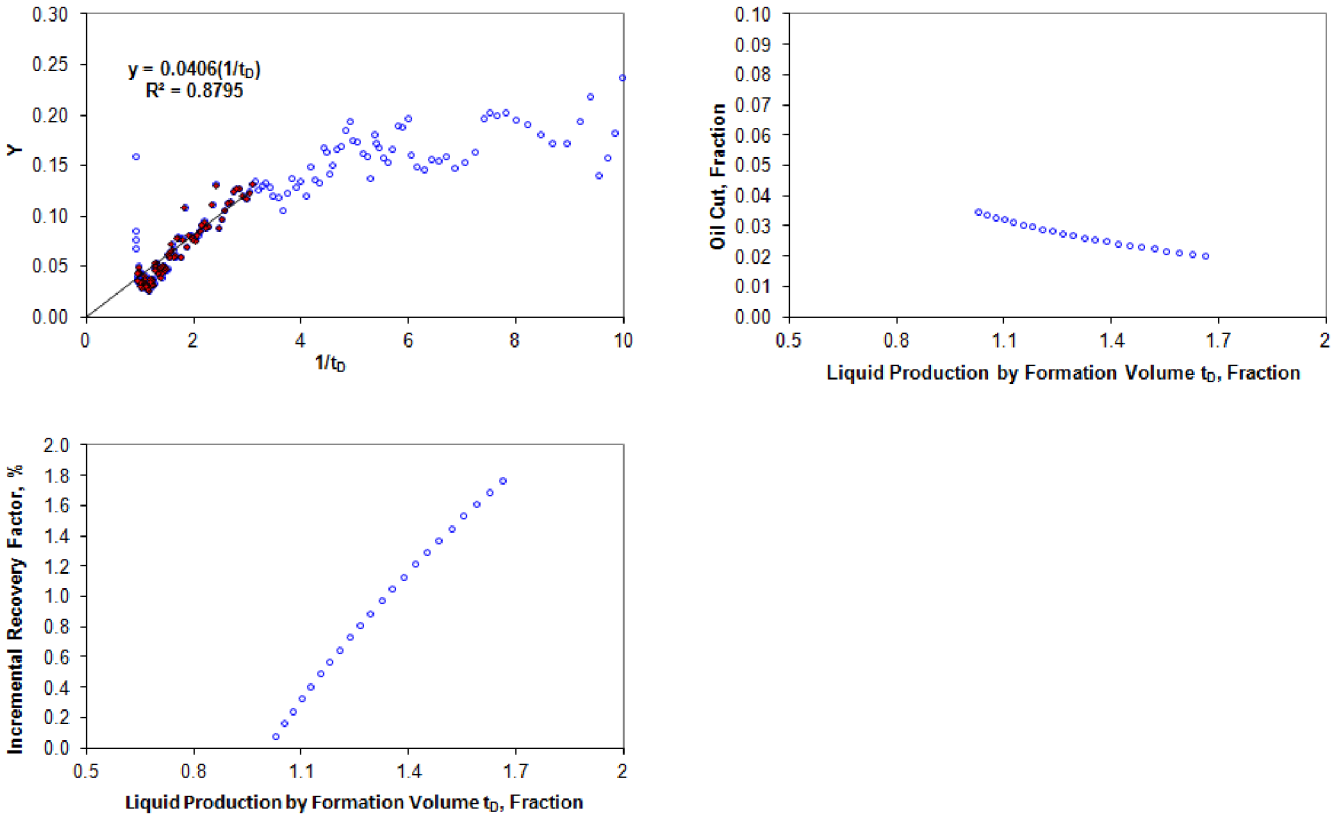

Figure 6—Area EE (reservoir D2) production data fitted by modified-Y plot (top left), forecasted oil cut vs. liquid production (top right), and estimated incremental recovery factor vs. liquid production (bottom left).

The capacitance-resistance method (CRM) is a simple, fast, yet powerful tool to quantify the reservoir and interwell connectivity based on the input of production and injection rates. Sayapour et. al (2007) introduced analytical solutions of CRM models in three different control volume sizes: (1) the volume of the entire field (CRMT), (2) the drainage volume of each producer (CRMP), and (3) the drainage volume between each injector-producer pair (CRMIP). In this study, the entire field level model (CRMT) was selected to evaluate reservoir connectivity. In Eq. (3), the CRMT equation presents the total fluid production from effects of primary recovery and water injection. In CRMT, field production rate $q(t_k)$ and injection rate $I_F(t_k)$ are routinely collected in the field and inputted into the model. With the objective function to minimize errors between actual and estimated field production rates, the outputs of Time Constant (τ) and Fraction of Injection (f_F) could be obtained. The time constant is a function of total compressibility, pore volume, and productivity index, while the fraction of injection is the ratio of total injected fluid volume travelling toward producers to total injected fluid volume. The fraction of injection is more focused in this study as it is a key indicator to understand the travelling direction of injected fluid. The CRMT model fits are shown in Figure 7 and the estimated f_F values for D2 and D3 reservoirs are 1 and 0.97, respectively. As the EE area is connected to the EK area, there is a possibility of fluid travelling across an arbitrary boundary. For D2 reservoir, some additional influx was anticipated as the estimated production rate remains lower than actual ones. Overall, high values of f_F confirm most injected water travelling toward producers.

$$q(t_k) = q(t_{k-1})e^{-\left(\frac{\Delta t_k}{\tau}\right)} + f_F I_F(t_k)\left(1 - e^{-\left(\frac{\Delta t_k}{\tau}\right)}\right) \quad (3)$$

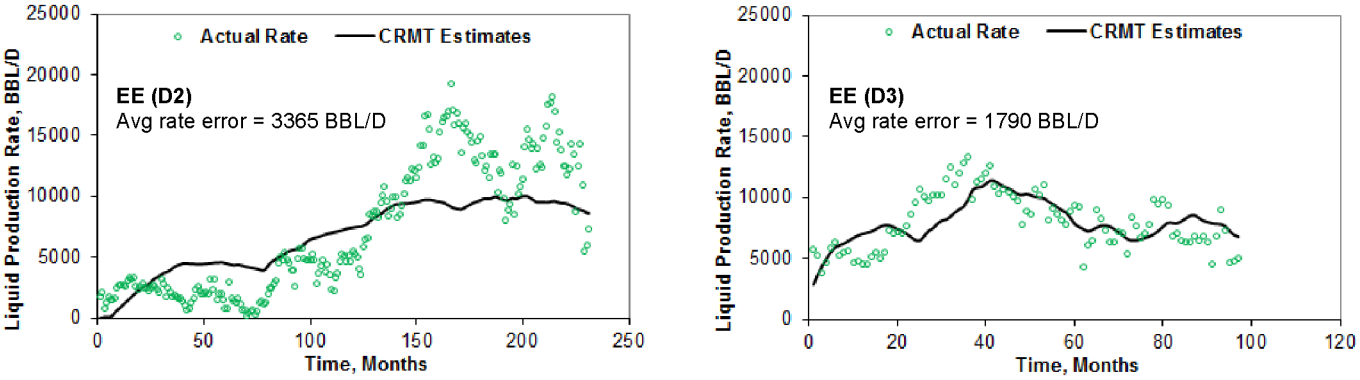

Figure 7—CRMT match of area EE reservoir D2 (left) and D3 (right) production rate.

Well Level Analysis

The well level analysis was performed to evaluate vertical heterogeneity and to monitor well injectivity in order to locate where waterflood performance is not promising. The common methods of heterogeneity measurement are Dykstra-Parsons coefficient and Lorenz plot. Dykstra and Parsons (1950) introduced the concept of permeability variation in a logarithmic plot. The Dykstra-Parsons equation for discrete multi-layers is shown in Eq. (4).

$$V_{DP} = \frac{\left(\frac{k_n}{\emptyset_n}\right)_{C_n=0.5} - \left(\frac{k_n}{\emptyset_n}\right)_{C_n=0.841}}{\left(\frac{k_n}{\emptyset_n}\right)_{C_n=0.5}} \tag{4}$$

The Lorenz coefficient is defined as the two times of area between flow capacity (FC) and storage capacity (C) and a 45° line (see example in Figure 8). The main inputs are porosity, permeability, and thickness of each layer. Therefore, the main source of data is routine core analysis (RCA) results from conventional coring, which is limitedly available in the S1 field due to the high operation cost associated. This study expands the usage of core data results to injection logging tool (ILT) results, which are routinely collected at every injector. The rotation speed of spinner is used to quantify injection rate and contribution into each reservoir layer and better represent flow capacity (FC) due to larger flow area of investigation. For storage capacity, information from wireline logging was selected to use. With this approach, it enables the calculation of Lorenz and Dykstra-Parsons coefficients at most injectors. In Figure 8, the calculation of Lorenz and Dykstra-Parsons coefficients at injector E03 are 0.55 and 0.73, respectively. In Figure 9, the vertical heterogeneity map was constructed from calculated Lorenz coefficients and injector locations to provide more insights into reservoir complexity distribution. The high vertical heterogeneity areas require more focus on conformance control, while the relatively low vertical heterogeneity area might be a good candidate for pilot EOR.

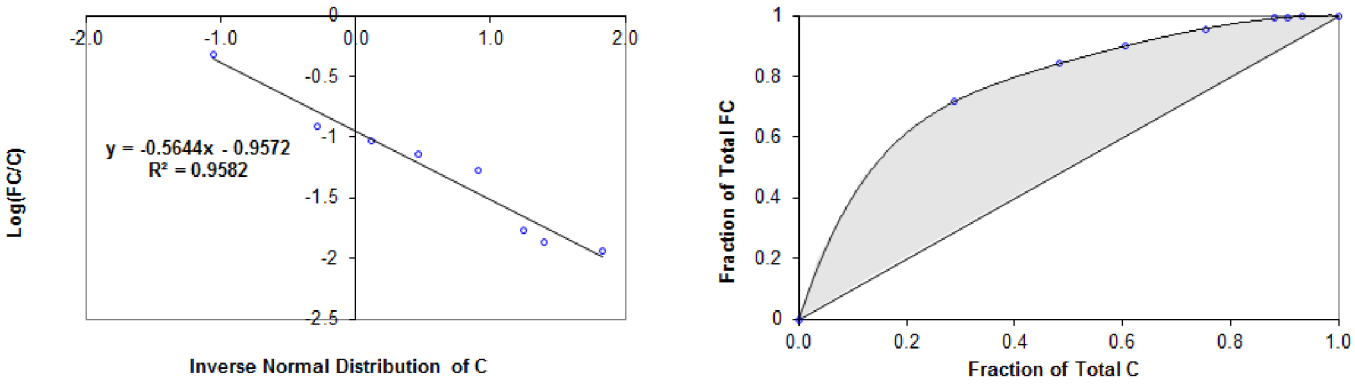

Figure 8—Dykstra-Parsons and Lorenz coefficient plots of E03 injector.

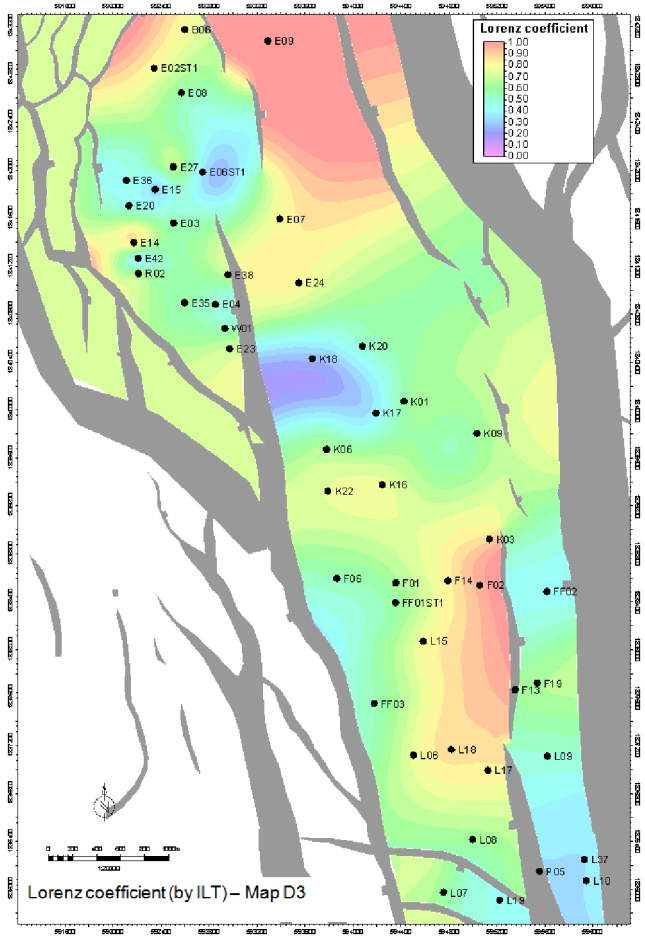

Figure 9—Vertical heterogeneity map constructed from Lorenz coefficients (using ILT data).

Hall's plot is a simple monitoring tool of well injectivity, which requires the inputs of injection rate, injection pressure, and reservoir pressure. Note that assumption of constant reservoir pressure was made here to simplify the method. The time integral of wellhead injection pressure (Y axis) is plotted with cumulative water injection (X axis). The slope indicates the reciprocal of well injectivity index; therefore, the upward and downward slope changes represent plugging and fracing conditions, respectively. To enhance the analysis, the interpretation needs to be carefully performed together with well activity log. In Figure 10, the Hall's plots suggest the evidences of plugging and fracing at injector E02. The well activity log supports the Hall's analysis because the sand plugging was indicated by shallower hold-up depth (HUD) when accessing with wireline. In addition, the fracing behavior happened after downhole plug was removed, which allowed

water to access into additional reservoirs. Obviously, the integration of Hall's plots and well activity log provides better understanding of well injectivity behaviors. On the other hand, E20 plot suggests neither plugging nor fracing issues. Overall, from 70% of total injectors in this area has experienced plugging issues, which are caused by sand and scale fill up (59%), injection zone change or isolation (27%), and other reasons including fish-in-hole and changing water source (14%). Treatment methods including sand clean out and acid wash have been performed to remedy the injectivity decline problem.

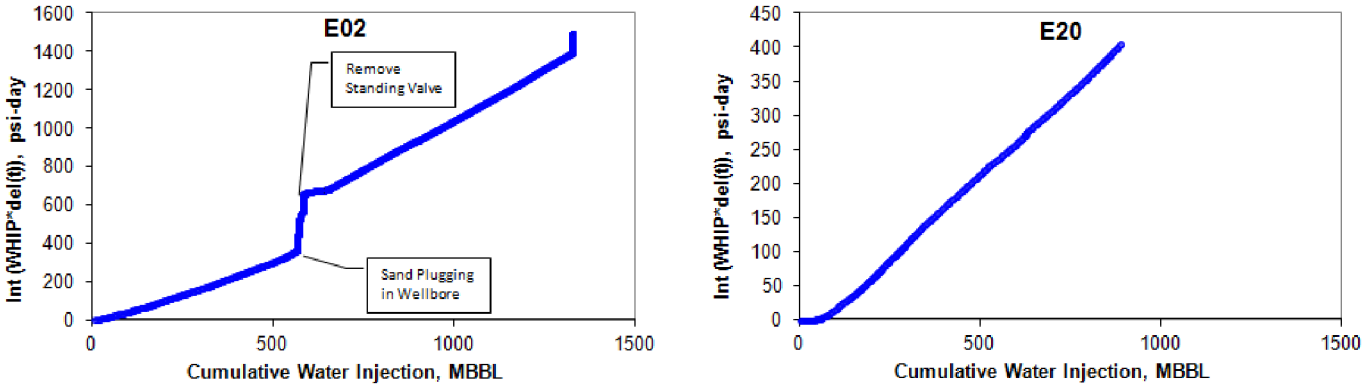

Figure 10—Hall plots indicate plugging and fracing issues at injector E02 (left) and no injection issue at injector E20 (right).

Discussion

The waterflood efficiency plots allow the comparison of waterflood performance among different areas. Different reservoir and waterflood design parameters were investigated in this study. It is proven that reservoirs with higher energy in depositional systems yield greater recovery from waterflood. The plots of recovery efficiency and cumulative water injection by pore volume help locate the areas with poorer waterflood performance, which require further investigation and specific mitigation plans. This plot can be used for analogous oil recovery gain in new areas. As shown in the recovery efficiency plot by reservoir drive mechanism, water injection has not been selected to implement in water drive reservoir because waterflood behaves in similar fashion as water displacement in water drive reservoir. Both efficiency plots by reservoir pressure when waterflood starts and reservoir drive mechanism confirm that the existence of free gas compromises waterflood efficiency mainly in terms of longer lead time for a reservoir fill-up period.

The integration of modified-Y plot with analytical recovery factor calculation and DCA method gives more prudent in reserves figure estimation. The different components of analytical recovery factor provide more insights into further improved oil recovery methods. For EE area, the microscopic and vertical displacement efficiency values are 0.59 and 0.70, respectively. The enhanced oil recovery techniques like water-alternating-gas (WAG) flooding, chemical EOR flooding, or conformance control agent injection will be further evaluated. The results from the CRMT model prove that most injected water (70%-100%) has been travelling toward producers.

In well level analysis, this study expands the usage of routine core analysis (RCA) data to injection logging tool (ILT) results in the vertical heterogeneity calculation. With the results from routine ILT operation, it enables the construction of vertical heterogeneity map, which shreds some lights on the distribution of reservoir complexity. From Hall's plot, the rigorous injection monitoring enables the spontaneous execution of well remedy program, which helps maintain the balance of injection and production in each area.

Conclusions

1. The recovery efficiency plots suggest the higher benefit of waterflood implementation in reservoirs with higher energy in a depositional system, depletion drive mechanism, and low level of pressure depletion.
2. The calculated analytical recovery factor can be used as a pre-screening tool of waterflood area selection, which can later be compared with the results from simulation, DCA, Modified-Y plot, or other methods to provide more confidence in reserves figures.
3. The constructed heterogeneity map improves the selection of further improved oil recovery methods and mitigation plan. Areas with high heterogeneity are likely to be a good candidate of conformance control, while those with low heterogeneity will be considered as a potential candidate for enhanced oil recovery (EOR).
4. The integration of Hall's plot and well operation log is used to spontaneously capture plugging and/or fracing behaviors as well as their possible root causes.

References

Craft, B.C. and Hawkins, M. 1991. *Applied Petroleum Reservoir Engineering*, second edition. Englewood Cliffs, New Jersey: Prentice Hall.

Fassihi, M. R. 1986. New Correlations for Calculation of Vertical Coverage and Areal Sweep Efficiency. *SPE Reservoir Engineering* (November 1986): 604–606.

Dykstra, H. and Parsons, R.L. 1950. The Prediction of Oil Recovery by Waterflooding. *Second Recovery of Oil in the United States*, second edition. New York: American Petroleum Institute.

Hall, H.N. 1963. How to Analyze Waterflood Injection Well Performance. *World Oil* (October 1963): 128–130.

Lake, L.W. 2010. *Enhanced Oil Recovery*. Richardson, Texas: Society of Petroleum Engineers.

Sahni, A., Dehghani, K., and Prieditis, J. 2005. Benchmarking Heterogeneity of Simulation Models. Presented at SPE Annual Technical Conference and Exhibition, Dallas, Texas, 9-12 October. SPE-96838.

Sayarpour, M., Zuluaga, E., Kabir, C.S., et al 2007. The Use of Capacitance-Resistive Models for Rapid Estimation of Waterflood Performance. Presented at SPE Annual Technical Conference and Exhibition, Anaheim, California, 11-14 November. SPE 110081-MS.

Terrado, M., Yudono, S., and Thakur, G. 2007. Waterflooding Surveillance and Monitoring: Putting Principles into Practice. Presented at SPE Annual Technical Conference and Exhibition, San Antonio, Texas, 24-27 September. SPE-102200.

Willhite, G. P. 1986. *Waterflooding*. Richardson: Society of Petroleum Engineers.

Yang, Z. 2009. A New Diagnostic Analysis Method for Waterflood Performance. *SPE Reservoir Evaluation and Engineering*(April 2009): 341–351.